# A method for continuous $^{239}$Pu determinations in Arctic and Antarctic ice cores

M. M. Arienzo[1*], J. R. McConnell[1], N. Chellman[1], A. S. Criscitiello[2], M. Curran[3,4], D. Fritzsche[5], S. Kipfstuhl[5], R. Mulvaney[6], M. Nolan[7], T. Opel[5], M. Sigl[8], J.P. Steffensen[9]

[1]Desert Research Institute, 2215 Raggio Parkway, Reno, NV, 33149, US

[2]University of Calgary, 2500 University Dr NW, Calgary, AB T2N 1N4, Canada

[3]Australian Antarctic Division, 203 Channel Highway, Kingston Tasmania 7050, Australia

[4]Antarctic Climate and Ecosystems Cooperative Research Centre, University of Tasmania, Hobart 7001, Australia.

[5]Alfred-Wegener-Institut, Potsdam/Bremerhaven, Germany

[6]British Antarctic Survey, High Cross, Madingley Road Cambridge, CB3 0ET, UK

[7]University of Alaska Fairbanks, 505 N Chandalar Dr, Fairbanks, AK, 99775, US

[8]Paul Scherrer Institute, 5232 Villigen, Switzerland

[9]Centre for Ice and Climate, Niels Bohr Institute, University of Copenhagen, Copenhagen, Denmark.

**CORRESPONDING AUTHOR**

* Desert Research Institute, 2215 Raggio Parkway, Reno, NV, 33149, US; Email: marienzo@dri.edu; Phone: 775-673-7693

## ABSTRACT

Atmospheric nuclear weapons testing (NWT) resulted in the injection of plutonium (Pu) into the atmosphere and subsequent global deposition. We present a new method for continuous semi-quantitative measurement of $^{239}$Pu in ice cores, which was used to develop annual records of fallout from NWT in ten ice cores from Greenland and Antarctica. The $^{239}$Pu was measured directly using an Inductively Coupled Plasma – Sector Field Mass Spectrometer, thereby reducing analysis time and increasing depth-resolution with respect to previous methods. To validate this method, we compared our one year averaged results to published $^{239}$Pu records and other records of NWT. The $^{239}$Pu profiles from four Arctic ice cores reflected global trends in NWT and were in agreement with discrete Pu profiles from lower latitude ice cores. The $^{239}$Pu measurements in the Antarctic ice cores tracked low latitude NWT, consistent with previously published discrete records from Antarctica. Advantages of the continuous $^{239}$Pu measurement method are (1) reduced sample preparation and analysis time; (2) no requirement for additional ice samples for NWT fallout determinations; (3) measurements are exactly co-registered with all other chemical, elemental, isotopic, and gas measurements from the continuous analytical system; and (4) the long half-life means the $^{239}$Pu record is stable through time.


## ABSTRACT ART

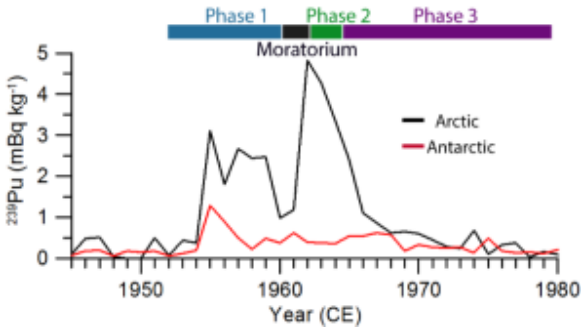

## 1. INTRODUCTION

The transuranic radioactive chemical element plutonium (Pu), first artificially produced in 1940, is present in the environment as a result of nuclear weapons testing (NWT) conducted from 1945 to 1980 Common Era (CE).[1] Plutonium primarily exists as six isotopes: $^{238}$Pu, $^{239}$Pu, $^{240}$Pu, $^{241}$Pu, $^{242}$Pu, and $^{244}$Pu, with $^{239}$Pu being the most abundant in the environment and $^{244}$Pu having the longest half-life. It is estimated that 6.5 PBq of $^{239}$Pu was released globally as a result of atmospheric NWT.[1]

Atmospheric nuclear weapons tests were primarily conducted in three major phases. Phase one occurred from 1952 to 1959 CE and was dominated by United States (U.S.) testing in the low latitude Pacific (Bikini, Eniwetok, and Johnston Islands) and in Nevada[1] (Figure 1). One of the largest tests conducted during this time was the Bravo test in February 1954 at Bikini Atoll, with a total yield of 15 Mt.[1] Other testing during this first period took place in the Pacific (Malden and Christmas Islands) and Australia by the United Kingdom (U.K.).[1] This period was followed by the Partial Test Ban moratorium from 1959 to 1961 CE. Phase two occurred from 1961 to 1962 CE and was dominated by testing conducted by the former Soviet Union (USSR) at Novaya Zemlya (Russian Arctic) and Semipalatinsk (Kazakhstan) (Figure 1). The largest Northern Hemisphere (NH) testing occurred over the Russian Arctic during this period, with the yield accounting for ~57% of all atmospheric NWT.[1, 2] Additional testing was conducted at the U.S. Pacific sites. In 1963 CE, the USSR and U.S. signed the Limited Test Ban Treaty in which the two countries stopped all aboveground testing. Phase three was dominated by 64 aboveground tests from 1960 to 1980 CE largely conducted by France and China. French testing was conducted in the Algerian Sahara and French Polynesia (Mururoa and Fangataufa Atolls)

63 while Chinese testing primarily was conducted in Lop Nor, western China[1] (Figure 1).
64 Radionuclide aerosols additionally were released during the Chernobyl accident in 1986 CE.[2]

65 Aerosols from NWT were dispersed on local, regional (tropospheric), or global
66 (stratospheric) scales. Aerosols emitted by NWT were partitioned depending on the altitude and
67 size of the test as well as the local meteorology,[1] and fallout occurred during periods ranging
68 from minutes to five years following the atmospheric tests.[3] Aerosols injected into the
69 stratosphere, which is thermally stratified from the troposphere, had the longest residence times.
70 Radionuclides were transported in the atmosphere from testing sites to the high latitude ice cores
71 sites in the stratosphere.[4] Radionuclides were transferred from the stratosphere to the troposphere
72 seasonally, which in the NH occurred during the late winter to spring.[4] Removal of Pu from the
73 atmosphere occurred either through wet (precipitation) or dry deposition,[2] and the greatest
74 surface deposition of radionuclide aerosols was in the NH temperate latitudes with only 20% of
75 the total fallout in the Southern Hemisphere (SH).[5]

76 Various chemical tracers have been utilized to reconstruct the transport and deposition of
77 radionuclides associated with NWT (i.e., $^{3}H$, $^{14}C$, $^{36}Cl$, $^{90}Sr$, $^{137}Cs$, $^{210}Pb$, $^{240}Pu/^{239}Pu$, total-beta).
78 Records of NWT have been developed from archives including vegetation and soil samples,[4, 6]
79 corals,[7, 8] air filters,[3, 9] lake sediments,[6, 10] polar ice cores,[2, 11-14] and mid-latitude ice cores.[15-19]
80 Proxies such as corals, lake sediments, and soils may exhibit post-depositional alteration, low
81 accumulation, and mixing,[6] while ice cores typically exhibit higher annual accumulation rates
82 and minimal post-depositional alteration or mixing. Ice cores have been successfully used to
83 reconstruct atmospheric transport and fallout of NWT.[2, 20] Measurements of $^{239}Pu$ also have the
84 potential to provide specific age tie points between various ice-core and other environmental
85 records.[11]

The chemical content of ice cores is a proxy for atmospheric aerosol composition and therefore historical changes. Because of the long half-life of $^{239}$Pu (24.2 ky), the records of $^{239}$Pu will be stable in ice cores through time, unlike beta-radiation-based methods. Due to the low concentration of Pu in the atmosphere and ice cores, sensitive instrumentation or large sample size is required for measurement. Traditional methods for analyzing Pu in ice cores include Accelerator Mass Spectrometry (AMS) which requires large dedicated sample sizes (hence reduced depth and temporal resolution, typically ~3 years) and is time consuming both for sample preparation and analysis.[16] Gabrieli et al.[15] achieved higher resolution using semi-quantitative Inductively Coupled Plasma – Sector Field Mass Spectrometry (ICP-SFMS equipped with a desolvation nebulizer) measurements of $^{239}$Pu in discrete samples from an ice core from the Swiss/Italian Alps. These measurements yielded a time resolution of 0.5 to 1.5 years while greatly reducing the time required for analysis.[15] Here we extend the ice core ICP-SFMS method from discrete to continuous, melter-based measurements using ICP-SFMS[21] – with the aim of minimizing sample requirements, sample handling, and decontamination efforts while maximizing depth resolution, measurement robustness and ensuring exact depth registration with all other chemical, elemental, isotopic, and gas measurements. We applied this new method to an array of ten annually dated ice cores from widely spaced sites both in Antarctica and Greenland (Figure 1) to develop an annual, semi-quantitative record of $^{239}$Pu deposition throughout the high latitudes, and evaluate this new method through comparison to previously published discrete $^{239}$Pu records. We also demonstrated the usefulness of this new method as a dating tool by applying the method to three additional ice cores from Alaska, the Russian Arctic, and Antarctica with lower confidence depth-age scales.

## 2. MATERIAL AND METHODS

## 2.1 Samples

Four Arctic and six Antarctic ice cores were analyzed for semi-quantitative $^{239}Pu$ concentrations (Table 1, Figure 1). All ten cores previously had been dated using annual layer counting of multiple seasonal chemical cycles in the ice, and the dating was constrained with volcanic synchronization to the timescale of Sigl et al.[22,23] The Arctic cores included D4,[24] Summit_2010, Tunu2013,[22] and NEEM-2011-S1[22] (Figure 1). The Antarctic cores are Aurora Basin North (ABN) and B40[25] from East Antarctica, James Ross Island[26] (JRI) from the Antarctic Peninsula, and Pine Island Glacier (PIG),[27] Thwaites Glacier (THW),[27] and the divide between Pine Island and Thwaites Glaciers (DIV)[27] from West Antarctica (Figure 1). Three additional ice cores from Alaska, the Russian Arctic, and Antarctica were also analyzed for $^{239}Pu$ and these samples consisted of lower confidence depth-age scales and will be discussed in detail in section 4.3.

## 2.2 Analytical Methods

Pu and a broad range of more than 20 elements and chemical species were analyzed using the Desert Research Institute's (DRI's) continuous melter system (adapted from McConnell et al.[21]) (Figure 2). For this study, methods and results will focus on $^{238}U$ and $^{239}Pu$. Prior to analysis, longitudinal samples with a cross section of ~0.032 by ~0.032 m from all ice cores were cut and the ends decontaminated by scraping with a pre-cleaned ceramic knife.[21, 28] The ice cores were melted continuously from bottom to top and a portion of the meltwater from the uncontaminated center of the longitudinal sample was introduced to a Thermo-Finnigan Element2 (Thermo Scientific, Bremen, Germany) ICP-SFMS approximately four minutes after melting. The continuous sample stream was acidified inline to 2% $HNO_3$, with $^{89}Y$ and $^{115}In$ added to the sample stream as external and internal standards, respectively (Figure 2). The ICP-SFMS was housed in a class-100 clean room, and the instrument outfitted with a cyclonic spray

133 chamber and a Teflon® PFA self-aspirating nebulizer (Elemental Scientific, Omaha, NE, USA)
134 for stable sample introduction. The tubing from the melter into the ICP-SFMS was acid cleaned
135 (1% $HNO_3$) at least twice daily.

136 The ICP-MS instrument measured a suite of elements continuously in low resolution
137 ($M/\Delta M = 300$)[21] (Figure 2). Therefore when conducting continuous elemental measurements of
138 ice cores, there is an inherent tradeoff between temporal resolution of the analyses (i.e. ice core
139 depth resolution) and measurement time spent on each element (Figure 2). With increased
140 measurement time spent on each element, the number of measurements per element would
141 increase, however the ice core depth resolution per element would decrease. This issue arises
142 when conducting continuous Pu measurements. For $^{239}Pu$ measurements, the magnet was fixed at
143 mass 238.050 with electric scanning (E-scan) between $^{238}U$ and $^{239}Pu$. The $^{239}Pu$ sample time was
144 0.4 s with 50 samples per peak (for 4 s total), and the $^{238}U$ sample time was 0.02 s with 50
145 samples per peak. Overall, instrument measurement of all elements consisted of an effective
146 sample rate of approximately 8 to 10 s (~6 mm sample depth). This approach allows for enough
147 measurement time to be spent on Pu to acquire robust measurements while maintaining the ice
148 core depth resolution for the additional elements. Ice core samples were not filtered, as particle
149 influences are minimal. Every ~2.5 hours during routine pauses in the continuous ice-core
150 analyses, procedural blanks were analyzed.

151 Similar to Gabrieli et al.,[15] we conducted an indirect calibration of $^{239}Pu$ utilizing $^{238}U$.
152 Five standards ranging in U concentration from 0.01 to 8.0 pg $g^{-1}$ were measured at the
153 beginning of each analysis day with quality control standards analyzed at the beginning and end
154 of the day. Standards were prepared from a 0.2 μg $g^{-1}$ multi-elemental stock solution (Inorganic
155 Ventures, Christiansburg, VA, USA) in ultrapure 1% $HNO_3$. Using the diluted standards, we

156 acquired a linear calibration curve and matrix matched the standards to the samples. As
157 demonstrated by Gabrieli et al.,[15] this method provides a first approximation since the Pu and U
158 ions behave similarly in the ICP-SFMS. From the semi-quantitative calibration, the $^{239}Pu$ results
159 were expressed in concentration and activity units, using the $^{239}Pu$ specific activity value from
160 Baglan et al.[29] of $2.29 \times 10^9$ Bq $g^{-1}$. Depositional flux of $^{239}Pu$ was calculated from $^{239}Pu$ activity
161 multiplied by each year's water-equivalent accumulation derived from annual-layer counting.
162 Since an indirect calibration was conducted $^{239}Pu$ concentration, activity and flux are semi-
163 quantitative.

164 One potential source of interference for $^{239}Pu$ is $^{238}UH^+$.[15] As shown by Gabrieli et al.,[15]
165 at low U concentrations (<40 pg $g^{-1}$) the $^{238}UH^+$ interferences were minimal and when
166 interferences were detected, the interferences were much greater than $^{239}Pu$ measurements. In
167 this study, the 1940 to 1985 CE average U concentration was ~0.25 pg $g^{-1}$ for the Greenland ice
168 cores and ~0.05 pg $g^{-1}$ for the Antarctic ice cores. Additionally co-variability between Pu and U
169 measurements was not observed for the Greenland or Antarctic ice cores between 1940 to 1985
170 CE. While the U cocentrations are low, to avoid potential $^{238}UH^+$ interferences impacting results,
171 the 4 s dwell for every 10 s sampling rate was averaged to one year intervals (~40 Pu
172 measurements $year^{-1}$) therefore reducing the measurement variability. To calculate the detection
173 limit, blanks were analyzed periodically throughout the continuous analyses. The blank results
174 were averaged to ~100 s intervals (~10 Pu measurements). The detection limit was then
175 calculated as three times the standard deviation of the blanks with an average value of ~0.24 fg $g^{-1}$
176 (~0.55 mBq $kg^{-1}$). After 60 s of blank washout, >90% of all U was removed, therefore memory
177 effects are thought to be minimal. Blank correction was made by averaging the sample $^{239}Pu$

178 value from 1900 to 1940 CE and subtracting from measured values. The average $^{239}$Pu for the ten
179 ice cores from 1900 to 1940 CE was 0.28 fg g$^{-1}$.

180 3. RESULTS

181 Here we report continuous measurements of $^{239}$Pu from four Arctic and six Antarctic ice
182 cores. All cores were previously dated with annual-layer counting with age uncertainties
183 typically ≤ 1 year. The $^{239}$Pu data are presented as yearly averages. Composite records for
184 concentration, activities, and fluxes were calculated from the geometric mean of the annual
185 averages.

186 In the Arctic, $^{239}$Pu was first detected in the ice cores in 1953 CE, followed by a peak in
187 1955 CE, a small decline in 1956 CE, and increased values to 1959 CE (Figure 3). The 1955 to
188 1959 CE period consisted of an average $^{239}$Pu semi-quantitative concentration of 1.1 fg g$^{-1}$ (2.5
189 mBq kg$^{-1}$). All ice cores exhibited a minimum from 1960 to 1961 CE, with an average
190 concentration of 0.5 fg g$^{-1}$ (1.1 mBq kg$^{-1}$). This was followed by a rapid increase in $^{239}$Pu
191 concentration from 1962 to 1965 CE, with average $^{239}$Pu values of 1.6 fg g$^{-1}$ (3.7 mBq kg$^{-1}$), and
192 the greatest $^{239}$Pu concentration (6.2 fg g$^{-1}$) was observed in the Tunu2013 ice core in 1962 CE.
193 The $^{239}$Pu concentration significantly declined by 1968 CE, with values returning to background
194 by ~1980 CE. The average standard error of the measurement from 1945 to 1985 CE was 0.2 fg
195 g$^{-1}$. Concentrations varied between sites because wet and dry deposition processes may have
196 differed with accumulation rates and other depositional processes, therefore the $^{239}$Pu activity
197 was converted to flux (Figure 3b). The D4 ice core had a greater accumulation rate and hence
198 greater $^{239}$Pu activity flux than the other Arctic ice cores, with an average value of 996 mBq m$^{-2}$
199 yr$^{-1}$ from 1953 to 1965 CE (Figure 3b). The average $^{239}$Pu activity flux for the four Arctic ice
200 cores from 1953 to 1965 CE was 500 mBq m$^{-2}$ yr$^{-1}$.

201 The semi-quantitative $^{239}$Pu activity measurements from six Antarctic ice cores are shown
202 in Figure 4a. Overall, $^{239}$Pu levels were lower than those observed in the Arctic. Increased
203 activities were observed from 1955 to 1957 CE (Figure 4a) with an average concentration of 0.4
204 fg g$^{-1}$ (0.9 mBq kg$^{-1}$) and the greatest concentration (1.2 fg g$^{-1}$) measured in the THW core in
205 1955 CE. After 1957 CE, $^{239}$Pu values declined followed by a peak in 1961 CE and a second
206 peak from 1967 to 1968 CE and a return to background by ~1975 CE. The average standard error
207 of the measurement from 1945 to 1985 CE was 0.1 fg g$^{-1}$ for the Antarctic ice cores. When
208 accounting for accumulation rate variations, the greatest $^{239}$Pu flux was observed at the DIV,
209 PIG, and THW cores, likely because of higher accumulation rate at these sites (Table 1, Figure
210 4b) with an average $^{239}$Pu flux of 250 mBq m$^{-2}$ yr$^{-1}$ from 1953 to 1965 CE. The average Antarctic
211 $^{239}$Pu flux for the six ice cores was 120 mBq m$^{-2}$ yr$^{-1}$ from 1953 to 1965 CE.

212 4. DISCUSSION

213 **4.1 Comparison to published NWT records**

214 To evaluate the $^{239}$Pu measurements, we compared composite ice-core records of $^{239}$Pu
215 activity to published total NWT fission yields[1] (Figure 5). The first significant atmospheric tests
216 were conducted in 1952 CE and included the Mike test in Eniwetok Atoll and the 1955 CE
217 Bravo test.[1] These tests were reflected in both the Arctic and Antarctic ice cores with the first
218 detection of $^{239}$Pu in 1953 CE and increased $^{239}$Pu from 1955 to 1959 CE dominated by the U.S.
219 tests in the low-latitude Pacific. With the largest tests conducted from 1952 to 1958 CE.[1] The
220 Partial Test Ban moratorium resulted in a decline in $^{239}$Pu, but values remained above baseline.
221 This has been shown in other ice cores[15] and is thought to be due to the longer residence time of
222 $^{239}$Pu in the atmosphere. Post-moratorium in the fall of 1961 CE, the USSR resumed tests
223 corresponding to a period of the most powerful testing, particularly at the Novaya Zemlya site
224 with a test in October 1961 CE with a total release of 50 Mt.[1] This increase in testing clearly was

225 reflected in the Arctic record, with the greatest measured values during the post-moratorium
226 (post-1961 CE) period. Unlike the Arctic, where the peak $^{239}$Pu concentration measurement
227 occurred during the early 1960s, after 1958 CE the Antarctic $^{239}$Pu record remained relatively
228 low, with only a slight increase in the early and late 1960s. Although the tests conducted in the
229 1960s were large, there was minimal transport from the Russian Arctic to Antarctica, hence the
230 low $^{239}$Pu. In 1963 CE, the Limited Test Ban Treaty was signed and $^{239}$Pu activity in both the
231 Arctic and Antarctic records began to decline. Activity remained above baseline, however, as
232 French and Chinese testing continued into the late 1970s. French testing in the South Pacific
233 Ocean in Fangataufa and Mururoa Islands peaked in 1968 CE, which was reflected in our
234 Antarctic records (Figure 5).

235 From 1953 to 1980 CE, more than 500 aboveground nuclear weapons tests resulted in
236 global fallout of $^{239}$Pu. With most of the testing conducted in the NH, the NH to SH ratio of $^{239}$Pu
237 fallout[4] was ~3:1, and similarly the average $^{239}$Pu activity for the Arctic and Antarctic ice cores
238 was 1.3 and 0.4 mBq kg$^{-1}$, respectively.

239 **4.2 Comparison to previously published records of fallout**

240 We performed further evaluation of the continuous $^{239}$Pu method by comparing the
241 Antarctic and Arctic composite records to previously published discrete $^{239}$Pu records. When
242 comparing to various ice-core records, overall good agreement was observed – expected given
243 that NWT aerosols were globally distributed – and provided greater confidence in the method
244 (Figure 6). Results from three Greenland sites (South Dome, Camp Century, and Dye-3) showed
245 increased $^{239}$Pu from 1955 to 1960 CE with greater values from 1963 to 1965 CE.[11, 30, 31] The
246 1965 CE $^{239}$Pu activity from South Dome[30, 32] was 9 ±0.3 d.p.h. kg$^{-1}$, similar to the average
247 activity of 2.4 mBq kg$^{-1}$ observed in Greenland from this study. The average value at Camp

Century[32] for the 1965 CE stratum, however, was higher at 11.3±0.3 d.p.h. $kg^{-1}$, potentially because of variations in flux. The $^{239}$Pu post-moratorium (1962 to 1965 CE) to pre-moratorium (1955 to 1959 CE) ratio was 59:41% for Dye-3, 56:44% for South Dome,[31] and 60:40% for this study. These ratios were offset from the 70:30% determined from the total atmospheric NWT, possibly due to variations in the type of weapons tested,[31] transport, or depositional processes.

With respect to lower latitude records, the Colle Gnifetti and Colle du Dome from the Alps both show two $^{239}$Pu peaks in the pre-moratorium period (1955 to 1959 CE) with a minimum in 1957 CE,[15] similar to the observations in the Arctic records (Figure 6). The records from UK herbarium specimens,[4] and ice cores from Belukha Glacier,[16] Colle Gnifetti,[15] and Colle du Dome[4] all demonstrate increased $^{239}$Pu activity post-moratorium (post-1961 CE).

Few studies have been conducted on Antarctic ice cores, but we observed generally favorable agreement with discrete $^{239}$Pu records from Antarctica. The $^{239}$Pu record from the Ross Ice Shelf showed a similar trend to the Antarctic ice-core records presented here, with the greatest $^{239}$Pu values observed from 1952 to 1955 CE (~8 d.p.h. $kg^{-1}$),[33] slightly higher than the peak values observed in this study. This was followed by a $^{239}$Pu activity peak of about half the size from 1962 to 1966 CE attributed to USSR and U.S. testing and an increase in the early 1970s attributed to French low-latitude testing.[33] Similar observations were made at Dome C with a large increase in $^{239}$Pu observed in 1956 CE (34 ±0.8 d.p.h. $kg^{-1}$) and significantly lower levels in the 1960s.[34] The $^{239}$Pu activity record from Dome C was greater than those observed here, but displayed a very similar overall trend.[32-34] The post-moratorium (1962 to 1965 CE) to pre-moratorium (1955 to 1959 CE) ratio for $^{239}$Pu was 36:64 % for Dome C, 57:43 % for the Ross Ice Sheet,[31] and for this study was 38:62 % (Figure 6).

### 4.3 Application of the continuous $^{239}$Pu method

271 Considering the favorable comparison between the well-dated ice cores to previously
272 published discrete records, we applied our method to ice cores with lower confidence depth-age
273 scales and compared the measurements to the Arctic and Antarctic $^{239}$Pu composite records
274 (Figure 7). Three additional cores were analyzed for $^{239}$Pu from sites where very low snow
275 accumulation and/or surface melting and percolation result in less distinct annual chemical
276 cycles and so lower confidence depth-age scales (Table 1). These additional cores included
277 McCall Glacier (McCallUC) from the Brooks Range, Alaska,[35] Akademii Nauk[36] from the
278 Russian Arctic, and a Norwegian/U.S. (NORUS) traverse core Site 8_5 from East
279 Antarctica[37](Figure 1).

280 The Akademii Nauk results from Severnaya Zemlya (Russian Arctic), located in close
281 proximity to the Russian Novaya Zemlya test site (Figure 1), showed increased $^{239}$Pu from 1953
282 to 1958 CE, with a peak value of 16 mBq kg$^{-1}$ in 1955 CE and no $^{239}$Pu increase in the post-
283 moratorium period (Figure 7b). This was similar to the $^{210}$Pb measurements on the same ice core
284 (Figure 7b) which showed a peak from 1953 to 1956 CE.[12] This is in contrast to the $^{137}$Cs activity
285 measurements from Akademii Nauk which peaked from 1962 to 1965 CE with a smaller increase
286 from 1953 to 1955 CE, in agreement with NWT records[12] (Figure 7b). The Austfonna ice core
287 record from Svalbard, sampled at a 3-5 year resolution, also contained one significant $^{239}$Pu peak
288 from 1956 to 1959 CE (Figure 6b). Considering the low Pu sampling resolution of the Austfonna
289 ice core record from Svalbard, care must be taken when interpreting this core. However,
290 previous studies propose that the deeper $^{239}$Pu from Austfonna[2] and the deeper $^{210}$Pb peak in
291 Akademii Nauk[12] are due to the percolation and migration of $^{239}$Pu and $^{210}$Pb during melt
292 periods.[2, 12, 36] This interpretation is potentially supported by the $^{239}$Pu measurements presented
293 here. Alternatively, the electrical conductivity and sulfate records for Akademii Nauk exhibited a

294 sharp increase at 1956 CE thought to be associated with the Bezymianny volcanic eruption.[36]
295 This suggests that the $^{210}$Pb and $^{239}$Pu records in Akademii Nauk may be impacted by dust
296 deposited during the volcanic event.[36] These results demonstrate that an ice core with high melt
297 and high amount of volcanic deposits may impact the $^{239}$Pu record.

298 The $^{239}$Pu record from McCallUC consisted of the greatest $^{239}$Pu activity measured
299 (Figure 7c). $^{239}$Pu was initially detected in 1946 CE and steadily increased to a peak in 1956 CE
300 of 13.6 mBq kg$^{-1}$. This was followed by a decline in 1957 CE and a second peak in 1959 CE.
301 Post-1961, $^{239}$Pu activities increased to 19 mBq kg$^{-1}$ in 1964 CE. Values in the McCallUC record
302 remained elevated until 1980 CE, when values returned to baseline. While the $^{239}$Pu activity was
303 much greater in McCallUC than found in the other cores analyzed here, the overall pattern was
304 similar to observed Greenland records, verifying the depth-age scale (Figure 7). The post-
305 moratorium (1962 to 1965 CE) to pre-moratorium (1955 to 1959 CE) ratio for $^{239}$Pu was 59:41%
306 for McCallUC, also similar to the Greenland records. The McCallUC site is a high dust site
307 potentially influenced by high northern latitude mining operations. Therefore, the greater $^{239}$Pu
308 activities measured in the McCallUC record may be impacted by the deposition of crustal dust
309 material contaminated with $^{239}$Pu or $^{238}$U, suggesting that care must be taken when applying this
310 method in high dust localities.[15]

311 The NORUS site 8_5 is a site of very low accumulation, however the $^{239}$Pu results agreed
312 well with the composite Antarctic record providing confidence in the age dating of this core. The
313 $^{239}$Pu record showed increased semi-quantitative $^{239}$Pu activity from 1953 to 1956 CE and lower
314 $^{239}$Pu activity post-moratorium (Figure 7d). The semi-quantitative $^{239}$Pu activity was much
315 greater than that measured at the other Antarctic sites due to the low accumulation rate (Table 1).

When accounting for variations in snowfall rates, the 1955 CE $^{239}$Pu activity flux was 130 mBq $m^{-2}$ $yr^{-1}$ for site 8_5, lower than the average 277 mBq $m^{-2}$ $yr^{-1}$ observed in Antarctica.

### 4.4 Environmental application

These results demonstrate the capabilities of the continuous ICP-SFMS $^{239}$Pu method when applied to ice cores. Here we produced two high latitude composite records of $^{239}$Pu applicable to the future evaluation and synchronization of ice cores chronologies, particularly for hard to date ice cores. While this method should be used with caution in high dust regions because of isobaric interferences from high U levels, our method for semi-quantitative $^{239}$Pu determinations provides an age constraint without the need for additional ice analyses. The continued application of this new method to a wide range of ice cores from varying localities may additionally shed light on lower latitude atmospheric aerosol sources and transport processes to the high latitudes.

FIGURE CAPTIONS

Figure 1: Ice cores analyzed in this study with well-constrained ages are shown as circles; ice cores with less constrained ages are shown as triangles. Black squares are $^{239}$Pu records previously published from U.K. herbarium samples,[4] and ice cores from Austfonna,[2] Colle du Dome near Mont Blanc,[4] Colle Gnifetti,[15] and Belukha Glacier.[16] Crosses indicate sites with significant NWT.[1]

Figure 2: Schematic of the ice-core melter, ICP-SFMS (left) and continuous flow analysis[21] (CFA) (right) systems, with examples of the types of elements and chemical species analyzed. The water pumped to the ICP-SFMS is from the center of the ice, and the flow path to both ICP-SFMS instruments is highlighted in red.

Figure 3: Annual average $^{239}$Pu results from the Arctic ice cores with well-constrained ages. (a) Semi-quantitative $^{239}$Pu activities and (b) semi-quantitative $^{239}$Pu activity fluxes for each of the ice cores with the composite geometric mean in black.

Figure 4: Annual average $^{239}$Pu results from the Antarctic ice cores with well-constrained ages. (a) Semi-quantitative $^{239}$Pu activities and (b) semi-quantitative $^{239}$Pu activity fluxes for each of the ice cores with the composite geometric mean in black.

Figure 5: Arctic (black) and Antarctic (red) composite semi-quantitative $^{239}$Pu activity compared to total NWT fission yields.[1] The NWT fission yields are divided by country and location of testing. Error bars represent the standard error of the mean.

Figure 6: Comparison to previously published $^{239}$Pu records. (a) Arctic mean (this study) (black), (b) $^{239}$Pu activity from Austfonna ice core (purple),[2] (c) Belukha Glacier ice core (light blue)[16], (d) herbarium samples collected in the U.K. (green),[4] (e) Colle du Dome ice core (orange),[4] (f) Colle Gnifetti ice core (blue),[15] and (g) Antarctic composite (this study) (red). Note the Colle du Dome $^{239}$Pu activity record is plotted on its own depth scale. Error bars are standard error of the mean.

Figure 7: Comparison between $^{239}$Pu activity records from well-dated ice cores and ice cores with less constrained age scales. (a) Arctic composite record, (b) Akademii Nauk ice core $^{239}$Pu activity (green), (c) McCallUC ice core (blue), (d) the Antarctic NORUS site 8_5 (purple), and (e) the Antarctic composite. Also shown are the Akademii Nauk $^{210}$Pb activity (orange) and $^{137}$Cs activity (brown) measurements from Pinglot et al.[12] Error bars are standard error of the mean.

360 TABLES AND FIGURES

| Site | Latitude (deg) | Longitude (deg) | Recent Accumulation kg $m^{-2}$ $y^{-1}$ |
|---|---|---|---|
| D4 | 71°24' N | 43°54' W | 414 |
| NEEM_2011_S1 | 77° 26' 56" N | 51° 03' 22" W | 204 |
| Summit 2010 | 72° 36' N | 38° 18' W | 221 |
| Tunu2013 | 78° 2' N | 33° 52' W | 112 |
| Akademii Nauk* | 80° 31' N | 94° 49' E | 423 |
| McCallUC* | 69° 18' N | 143° 48' W | 546 |
| ABN | 72° 00' S | 110° 00' E | 109 |
| B40 | 75° 0' S | 0°3'36" E | 68 |
| DIV | 76° 46' 13" S | 101° 44' 15" W | 372 |
| JRI | 64° 12' S | 57° 42' W | 595 |
| PIG | 77° 57' 25" S | 95° 57' 42" W | 400 |
| THW | 76° 57' 9" S | 121° 13' 13" W | 274 |
| Site_8_5* | 82° 38' S | 17° 52' E | 35 |

361

362 Table 1: Arctic and Antarctic sites used in this study. *Indicates records with lower confidence
363 depth-age scales.

364

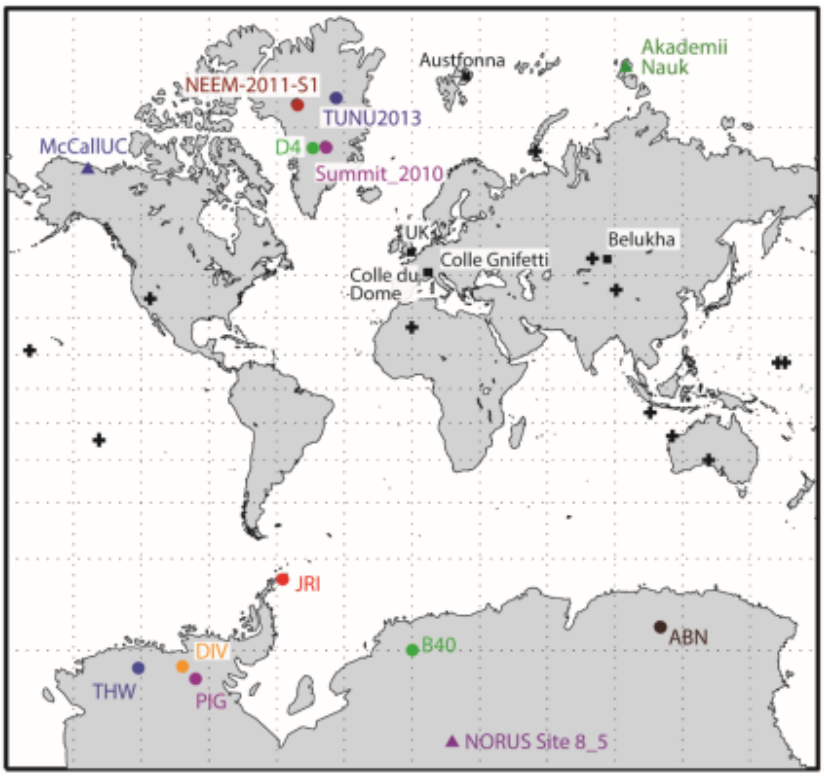


Figure 1: Ice cores analyzed in this study with well-constrained ages are shown as circles; ice cores with less constrained ages are shown as triangles. Black squares are $^{239}$Pu records previously published from U.K. herbarium samples,[4] and ice cores from Austfonna,[2] Colle du Dome near Mont Blanc,[4] Colle Gnifetti,[15] and Belukha Glacier.[16] Crosses indicate sites with significant NWT.[1]

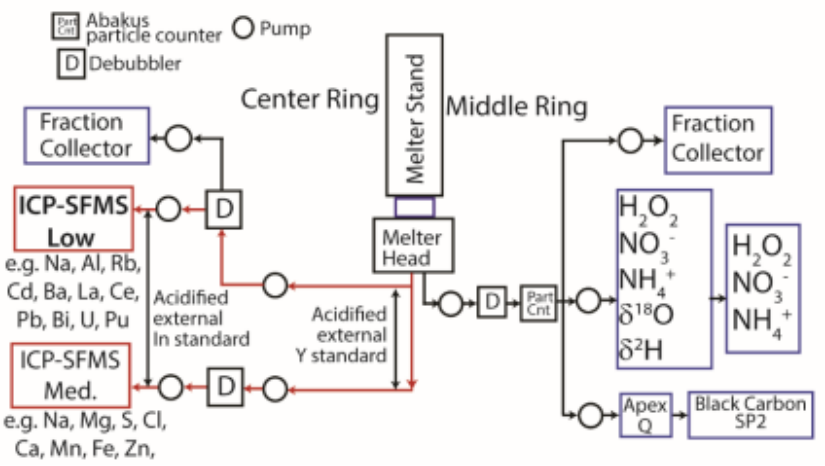


Figure 2: Schematic of the ice-core melter, ICP-SFMS (left) and continuous flow analysis[21] (CFA) (right) systems, with examples of the types of elements and chemical species analyzed. The water pumped to the ICP-SFMS is from the center of the ice, and the flow path to both ICP-SFMS instruments is highlighted in red.

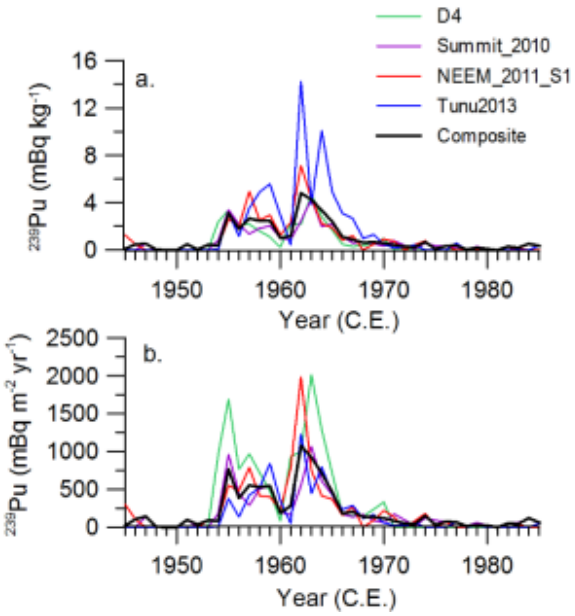


382

383 Figure 3: Annual average $^{239}$Pu results from the Arctic ice cores with well-constrained ages. (a)
384 Semi-quantitative $^{239}$Pu activities and (b) semi-quantitative $^{239}$Pu activity fluxes for each of the
385 ice cores with the composite geometric mean in black.

386

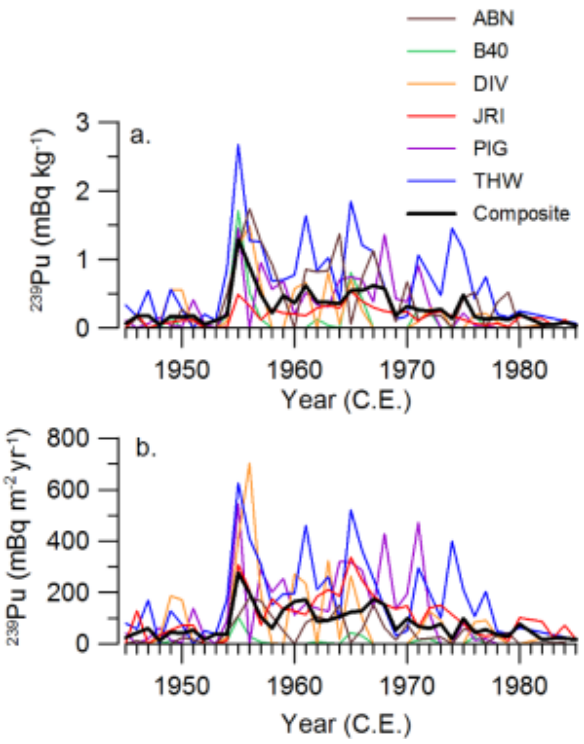


Figure 4: Annual average $^{239}$Pu results from the Antarctic ice cores with well-constrained ages. (a) Semi-quantitative $^{239}$Pu activities and (b) semi-quantitative $^{239}$Pu activity fluxes for each of the ice cores with the composite geometric mean in black.

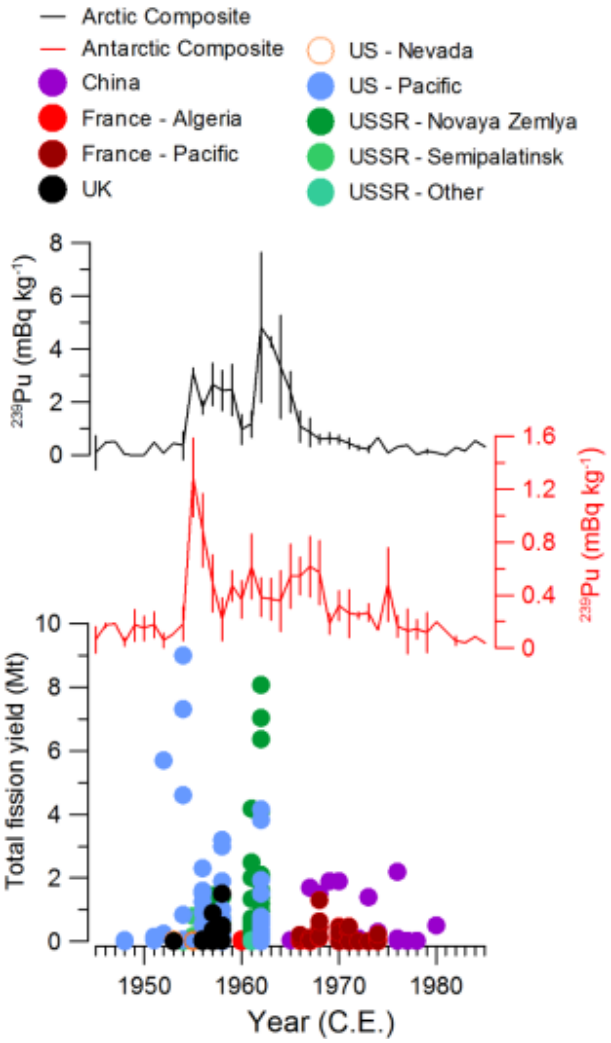


Figure 5: Arctic (black) and Antarctic (red) composite semi-quantitative $^{239}$Pu activity compared to total NWT fission yields.[1] The NWT fission yields are divided by country and location of testing. Error bars represent the standard error of the mean.

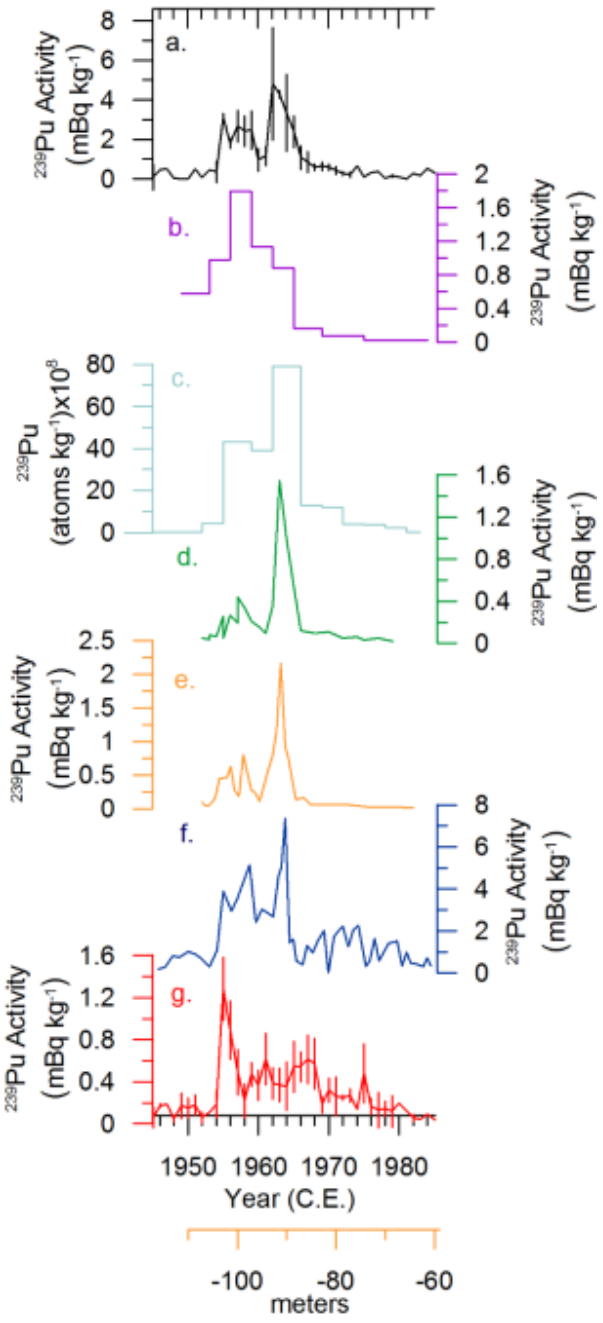


399

400 Figure 6: Comparison to previously published $^{239}$Pu records. (a) Arctic mean (this study) (black),
401 (b) $^{239}$Pu activity from Austfonna ice core (purple),[2] (c) Belukha Glacier ice core (light blue)[16],
402 (d) herbarium samples collected in the U.K. (green),[4] (e) Colle du Dome ice core (orange),[4] (f)
403 Colle Gnifetti ice core (blue),[15] and (g) Antarctic composite (this study) (red). Note the Colle du
404 Dome $^{239}$Pu activity record is plotted on its own depth scale. Error bars are standard error of the
405 mean.

406

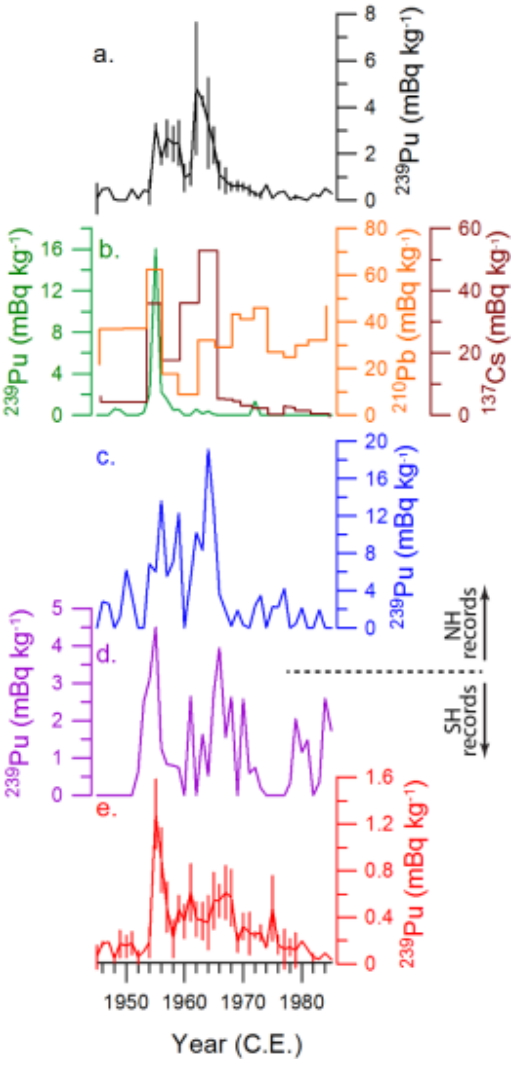


Figure 7: Comparison between $^{239}$Pu activity records from well-dated ice cores and ice cores with less constrained age scales. (a) Arctic composite record, (b) Akademii Nauk ice core $^{239}$Pu activity (green), (c) McCallUC ice core (blue), (d) the Antarctic NORUS site 8_5 (purple), and (e) the Antarctic composite. Also shown are the Akademii Nauk $^{210}$Pb activity (orange) and $^{137}$Cs activity (brown) measurements from Pinglot et al.[12] Error bars are standard error of the mean.

ACKNOWLEDGMENTS

The authors would like to thank those who aided with the organization, drilling, processing and analysis in the field and laboratory. We acknowledge L. Layman for his initial laboratory work and R. Kreidberg for his editorial advice. The authors would also like to thank the three anonymous reviewers for their constructive feedback. The following US NSF PLR grants supported collection and analyses of the cores as well as interpretation of the measurements: 0538416, 0856845, 0968391, 0909541, 1023672, 1023318, and 1204176. Ice-core data ($^{239}$Pu) for all ice cores are accessible at a data repository (to be determined).

## REFERENCES


1. UNSCEAR, Annex C: Exposures to the public from man-made sources of radiation. In *Sources and Effects of Ionizing Radiation*, Vienna, 2000.
2. Wendel, C.; Oughton, D.; Lind, O.; Skipperud, L.; Fifield, L.; Isaksson, E.; Tims, S.; Salbu, B., Chronology of Pu isotopes and $^{236}$U in an Arctic ice core. *Science of the Total Environment* **2013,** *461*, 734-741.
3. Alvarado, J.; Steinmann, P.; Estier, S.; Bochud, F.; Haldimann, M.; Froidevaux, P., Anthropogenic radionuclides in atmospheric air over Switzerland during the last few decades. *Nature Communications* **2014,** *5*, (3030), 1-6.
4. Warneke, T.; Croudace, I.; Warwick, P.; Taylor, R., A new ground-level fallout record of uranium and plutonium isotopes for northern temperate latitudes. *Earth and Planetary Science Letters* **2002,** *203*, (3-4), 1047-1057.
5. Hardy, E.; Krey, P.; Volchok, H., Global inventory and distribution of fallout Plutonium. *Nature* **1973,** *241*, (5390), 444-445.
6. Roos, P.; Holm, E.; Persson, R.; Aarkrog, A.; Nielsen, S., Deposition of $^{210}$Pb, $^{137}$Cs, $^{239+240}$Pu, $^{238}$Pu, and $^{241}$Am in the Antarctic Peninsula area. *Journal of Environmental Radioactivity* **1994,** *24*, 235--251.
7. Benninger, L.; Dodge, R., Fallout plutonium and natural radionuclides in annual bands of the coral Montastrea annularis, St. Croix, U.S. Virgin Islands. *Geochimica Et Cosmochimica Acta* **1986,** *50*, (12), 2785–2797.
8. Lindahl, P.; Asami, R.; Iryu, Y.; Worsfold, P.; Keith-Roach, M.; Choi, M., Sources of plutonium to the tropical Northwest Pacific Ocean (1943-1999) identified using a natural coral archive. *Geochimica Et Cosmochimica Acta* **2011,** *75*, (5), 1346-1356.
9. Wendel, C.; Fifield, L.; Oughton, D.; Lind, O.; Skipperud, L.; Bartnicki, J.; Tims, S.; Hoibraten, S.; Salbu, B., Long-range tropospheric transport of uranium and plutonium weapons fallout from Semipalatinsk nuclear test site to Norway. *Environment International* **2013,** *59*, 92-102.
10. Pennington, W.; Tutin, T. G.; Cambray, R. S.; Fisher, E. M., Observations on lake sediments using fallout $^{137}$Cs as a tracer. *Nature* **1973,** *242*, (5396), 324-326.
11. Koide, M.; Bertine, K.; Chow, T.; Goldberg, E., The $^{240}$Pu/$^{239}$Pu ratio, a potential geochronometer. *Earth and Planetary Science Letters* **1985,** *72*, (1), 1-8.
12. Pinglot, J.; Vaikmae, R.; Kamiyama, K.; Igarashi, M.; Fritzsche, D.; Wilhelms, F.; Koerner, R.; Henderson, L.; Isaksson, E.; Winther, J.; Van de Wal, R.; Fournier, M.; Bouisset, P.; Meijer, H., Ice cores from Arctic sub-polar glaciers: chronology and post-depositional processes deduced from radioactivity measurements. *Journal of Glaciology* **2003,** *49*, (164), 149-158.
13. Elmore, D.; Tubbs, L.; Newman, D.; Ma, X.; Finkel, R.; Nishizumi, K.; Beer, J.; Oeschger, H.; Andree, M., $^{36}$Cl bomb pulse measured in a shallow ice core from Dye-3, Greenland. *Nature* **1982,** *300*, (5894), 735-737.
14. Kotzer, T. G.; Kudo, A.; Zheng, J.; Workman, W., Natural and anthropogenic levels of tritium in a Canadian Arctic ice core, Agassiz Ice Cap, Ellesmere Island, and comparison with other radionuclides. *Journal of Glaciology* **2000,** *46*, (152), 35-40.
15. Gabrieli, J.; Cozzi, G.; Vallelonga, P.; Schwikowski, M.; Sigl, M.; Eickenberg, J.; Wacker, L.; Boutron, C.; Gaggeler, H.; Cescon, P.; Barbante, C., Contamination of Alpine snow and ice at Colle Gnifetti, Swiss/Italian Alps, from nuclear weapons tests. *Atmospheric Environment* **2011,** *45*, (3), 587-593.
16. Olivier, S.; Bajo, S.; Fifield, L.; Gaggeler, H.; Papina, T.; Santschi, P.; Schotterer, U.; Schwikowski, M.; Wacker, L., Plutonium from global fallout recorded in an ice core from the Belukha glacier, Siberian Altai. *Environmental Science & Technology* **2004,** *38*, (24), 6507-6512.
17. Schwikowski, M.; Brutsch, S.; Gaggeler, H.; Schotterer, U., A high-resolution air chemistry record from an Alpine ice core: Fiescherhorn glacier, Swiss Alps. *Journal of Geophysical Research-Atmospheres* **1999,** *104*, (D11), 13709-13719.

18. Naftz, D.; Klusman, R.; Michel, R.; Schuster, P.; Reddy, M.; Taylor, H.; Yanosky, T.; McConnaughey, E., Little Ice Age evidence from a south-central North America ice core, USA. *Arctic and Alpine Research* **1996,** *28*, (1), 35-41.
19. Knusel, S.; Ginot, P.; Schotterer, U.; Schwikowski, M.; Gaggeler, H.; Francou, B.; Petit, J.; Simoes, J.; Taupin, J., Dating of two nearby ice cores from the Illimani, Bolivia. *Journal of Geophysical Research-Atmospheres* **2003,** *108*, (D6), 1-11.
20. Fourre, E.; Jean-Baptiste, P.; Dapoigny, A.; Baumier, D.; Petit, J.; Jouzel, J., Past and recent tritium levels in Arctic and Antarctic polar caps. *Earth and Planetary Science Letters* **2006,** *245*, (1-2), 56-64.
21. McConnell, J.; Lamorey, G.; Lambert, S.; Taylor, K., Continuous ice-core chemical analyses using Inductively Coupled Plasma Mass Spectrometry. *Environmental Science & Technology* **2002,** *36*, (1), 7-11.
22. Sigl, M.; Winstrup, M.; McConnell, J.; Welten, K.; Plunkett, G.; Ludlow, F.; Büntgen, U.; Caffee, M.; Chellman, N.; Dahl-Jensen, D.; Fischer, H.; Kipfstuhl, S.; Kostick, C.; Maselli, O.; Mekhaldi, F.; Mulvaney, R.; Muscheler, R.; Pasteris, D.; Pilcher, J.; Salzer, M.; Schüpbach, S.; Steffensen, J.; Vinther, B.; Woodruff, T., Timing and climate forcing of volcanic eruptions for the past 2,500 years. *Nature* **2015,** *523*, 543–549.
23. Sigl, M.; Ferris, D.; Fudge, T. J.; Winstrup, M.; Cole-Dai, J.; McConnell, J. R.; Taylor, K. C.; Welten, K.; Woodruff, T. E.; Adolphi, F.; Brook, E. J.; Buizert, C.; Caffee, M. W.; Dunbar, N.; Geng, L.; Iverson, N.; Koffman, B.; Maselli, O. J.; McGwiew, K.; Muscheler, R.; Nishiizumi, K.; Pasteris, D. R.; Rhodes, R. H.; Sowers, T.; Svensson, A., The WAIS Divide deep ice core WD2014 chronology - Part 2: Annual-layer counting (0–31 ka BP). *Climate of the Past Discussions* **2015,** *11*, 3425-3474.
24. McConnell, J.; Edwards, R.; Kok, G.; Flanner, M.; Zender, C.; Saltzman, E.; Banta, J.; Pasteris, D.; Carter, M.; Kahl, J., 20th-century industrial black carbon emissions altered Arctic climate forcing. *Science* **2007,** *317*, (5843), 1381-4.
25. McConnell, J.; Maselli, O.; Sigl, M.; Vallelonga, P.; Neumann, T.; Anschutz, H.; Bales, R.; Curran, M.; Das, S.; Edwards, R.; Kipfstuhl, S.; Layman, L.; Thomas, E., Antarctic-wide array of high-resolution ice core records reveals pervasive lead pollution began in 1889 and persists today. *Scientific Reports* **2014,** *4*, 1-5.
26. Mulvaney, R.; Abram, N.; Hindmarsh, R.; Arrowsmith, C.; Fleet, L.; Triest, J.; Sime, L.; Alemany, O.; Foord, S., Recent Antarctic Peninsula warming relative to Holocene climate and ice-shelf history. *Nature* **2012,** *489*, (7414), 141-U204.
27. Criscitiello, A.; Das, S.; Karnauskas, K.; Evans, M.; Frey, K.; Joughin, I.; Steig, E.; McConnell, J.; Medley, B., Tropical Pacific influence on the source and transport of marine aerosols to West Antarctica. *Journal of Climate* **2014,** *27*, (3), 1343-1363.
28. Pasteris, D.; McConnell, J.; Edwards, R., High-resolution, continuous method for measurement of acidity in ice cores. *Environmental Science & Technology* **2012,** *46*, (3), 1659-1666.
29. Baglan, N.; Cossonnet, C.; Pitet, P.; Cavadore, D.; Exmelin, L.; Berard, P., On the use of ICP-MS for measuring plutonium in urine. *Journal of Radioanalytical and Nuclear Chemistry* **2000,** *243*, (2), 397-401.
30. Koide, M.; Goldberg, E.; Herron, M.; Langway, C., Transuranic depositional history in South Greenland firn layers. *Nature* **1977,** *269*, (5624), 137-139.
31. Koide, M.; Michel, R.; Goldberg, E.; Herron, M.; Langway, C., Characterization of radioactive fallout from pre-moratorium and post-moratorium tests to polar ice caps. *Nature* **1982,** *296*, (5857), 544-547.
32. Koide, M.; Goldberg, E., $^{241}Pu/^{239+240}Pu$ ratios in polar glaciers. *Earth and Planetary Science Letters* **1981,** *54*, (2), 239-247.
33. Koide, M.; Michel, R.; Goldberg, E.; Herron, M.; Langway, C., Depositional history of artificial radionuclides in the Ross Ice Shelf, Antarctica. *Earth and Planetary Science Letters* **1979,** *44*, 205-223.
34. Cutter, G.; Bruland, K.; Risebrough, R., Deposition and accumulation of plutonium isotopes in Antarctica. *Nature* **1979,** *279*, (5714), 628-629.

35. Nolan, M.; Arendt, A.; Rabus, B.; Hinzman, L.; Dowdeswell, J.; Willis, I., Volume change of McCall Glacier, Arctic Alaska, USA, 1956-2003. *Annals of Glaciology, Vol 42, 2005* **2005,** *42*, 409-416.
36. Fritzsche, D.; Wilhelms, F.; Savatyugin, L.; Pinglot, J.; Meyer, H.; Hubberten, H.; Miller, H., A new deep ice core from Akademii Nauk ice cap, Severnaya Zemlya, Eurasian Arctic: first results. *Annals of Glaciology, Vol 35* **2002,** *35*, 25-28.
37. Pasteris, D.; McConnell, J.; Edwards, R.; Isaksson, E.; Albert, M., Acidity decline in Antarctic ice cores during the Little Ice Age linked to changes in atmospheric nitrate and sea salt concentrations. *Journal of Geophysical Research-Atmospheres* **2014,** *119*, (9), 5640-5652.